

# Nonlocal-strain gradient forced vibration analysis of metal foam nanoplates with uniform and graded porosities

Mohammad Reza Barati\*

Aerospace Engineering Department & Center of Excellence in Computational Aerospace,  
Amirkabir University of Technology, Tehran, Iran

(Received July 01, 2017, Revised August 10, 2017, Accepted August 18, 2017)

**Abstract.** Forced vibration behavior of porous metal foam nanoplates on elastic medium is studied via a 4-variable plate theory. Different porosity distributions called uniform, symmetric and asymmetric are considered. Nonlocal strain gradient theory (NSGT) containing two scale parameters is employed for size-dependent modeling of porous nanoplates. The present plate theory satisfies the shear deformation effect and it has lower field variables compared with first order plate theory. Hamilton's principle is employed to derive the governing equations. Obtained results from Galerkin's method are verified with those provided in the literature. The effects of nonlocal parameter, strain gradient, foundation parameters, dynamic loading, porosity distributions and porosity coefficient on dynamic deflection and resonance frequencies of metal foam nanoscale plates are examined.

**Keywords:** forced vibration; 4-unknown plate theory; porous nanoplate; nonlocal elasticity; porosities

## 1. Introduction

Lightweight materials have been broadly applied in many engineering sciences due to their eligible stiffness with respect to their weight. Porous materials, such as metal foams, are an important category of lightweight materials with application to aerospace engineering, automotive industry and civil constructions owing to supreme multi-functionality offered by low specific weight, efficient capacity of energy dissipation and enhanced machinability. Usually, the variation of porosity through the thickness of porous plates causes a smooth change in mechanical properties. Therefore, this type of materials has received broad interest by some researchers.

Jabbari *et al.* (2013) examined porosity distribution effect on buckling characteristics of saturated porous plates. Chen *et al.* (2015) studied static bending and buckling of metal foam porous beams with functionally graded porosities using a shear deformation beam model. In another work, Chen *et al.* (2016) explored linear and nonlinear vibration behavior of metal foam beams with different porosity distributions. They stated that uniform and non-uniform porosity distributions have a significant influence on vibration frequencies of the plates due to the reduction in their stiffness.

Distinguished from the investigations related to the uniform and graded (non-uniform) porosity distribution effects on mechanical characteristics of metal foam beams and plates, some studies

---

\*Corresponding author, Ph.D., E-mail: [mrb.barati@ymail.com](mailto:mrb.barati@ymail.com)

have been performed on porous ceramic-metal or porous functionally graded (FG) structures. The latter is a different case in which the material properties are graded in the thickness direction based on the well-known power-law model considering the volume fraction of porosities. For example, Wattanasakulpong and Ungbhakorn (2014) employed a modified power-law function to describe the FG material properties with application to vibration analysis of porous beams. Also, Atmane *et al.* (2015) explored vibration and buckling characteristics of FG beams having porosities using higher order shear deformation theories.

Moreover, considerable progression in the utilization of structural elements such as beams and plates with micro and nano scales in micro/nano electro-mechanical systems (MEMS/NEMS), due to providing outstanding mechanical, chemical, and electronic characteristics, led to a sudden momentum in modeling of micro and nano scale structures. In these applications, size effects become prominent. The problem in using the classical theory is that the classical continuum mechanics theory does not take into account the size influence in nanosize structures. The classical continuum mechanics over predicts the responses of micro/nano structures. So a new form of continuum mechanics that captures small scale effect is required. The most commonly used continuum mechanics theory is proposed by Eringen (1983) known as nonlocal theory of elasticity. The theory includes the influences of small size with good accuracy to model micro/nano scale devices and systems. Several studies have been conducted extending nonlocal model to predict the mechanical responses of the nanostructures (Eltaher *et al.* 2016, Natarajan *et al.* 2012, Elmerabet *et al.* 2017, Tounsi *et al.* 2013, Barati *et al.* 2016, Zenkour and Abouelregal 2015, Kheroubi *et al.* 2016, Sobhy and Radwan 2017, Li *et al.* 2016a, Besseghier *et al.* 2015, Ebrahimi and Barati 2016, 2017a).

Searching the literature reveals that there is no published paper on metal foam nanoplates with the effect of porosity distribution. However, there are some published papers on analysis of mechanical behaviors of porous FG nanostructures based on modified power-law function. Mechab *et al.* (2016) examined vibrational characteristics of porous FG nanoplates resting on elastic medium using a higher order refined plate theory. Barati (2017a) explored forced vibration behavior of FG nanobeams with porosities under dynamic loads and resting on an elastic foundation. In another study, Ebrahimi and Barati (2017b) presented vibration analysis of porous FG nanobeams under magneto-electric field.

It is known that the Mindlin's plate theory suggests a displacement field having a linear configuration involving shear correction factors. Reddy (1984) proposed a third-order plate model which satisfies the lateral shear strains without the need for shear correction coefficients. Even though, new HSDTs possessing four field variables can produce sufficiently accurate results (Park *et al.* 2016, Javed *et al.* 2016, Becheri *et al.* 2016). The proposed theory contain fewer unknowns and equations of motion than the first-order and third order shear deformation theories, but satisfy the equilibrium conditions at the top and bottom surfaces of the plate without using any shear correction factors. Indeed, unlike the previous mentioned theories, the governing equations in the present theory are similar to the CPT.

Recently, nonlocal strain gradient theory (NSGT) is developed to consider both stiffness reduction and stiffness enhancement mechanisms in modeling and analysis of nanostructures (Lim *et al.* 2015). In fact, NSGT is a more reliable theory compared with nonlocal elasticity theory (NET) in which strain gradient effects have been ignored. Therefore, nonlocal elasticity theory used in previous studied is impotent to capture microstructure-dependent or strain gradient based behavior of nanoscale structures. In last two years, the works of present author and some other researchers is focused on the mechanical analysis of nanostructures (Barati and Zenkour 2017, Li

and Hu 2016, Li *et al.* 2016b, Xiao *et al.* 2017, Zhou and Li 2017).

In this research, forced vibration analysis of double-layered metal foam nanoplates with porosities is carried out applying a 4-unknown plate model considering exact location of neutral surface and different porosity distributions. Size-dependency of nanoplate is describe via a general nonlocal strain gradient theory with two scale parameters. Uniform, symmetric and asymmetric distributions of porosity have been considered. The present non-polynomial shear deformation theory possesses only four field variables and doesn't require a correction factor. Galerkin's approach is implemented to solve the governing equations. It is shown that the dynamic deflection and resonance frequencies of porous nanoplates are significantly affected by porosities coefficient, porosity distribution, nonlocality, strain gradients, elastic foundation constants and dynamic loading.

### 2. Modeling of nanoplates based on NSGT

Based on NSGT, the stress field is divided into a nonlocal stress  $\sigma_{ij}^{(0)}$  and a higher order stress field  $\nabla\sigma_{ij}^{(1)}$  as (Barati and Zenkour 2017)

$$\sigma_{ij} = \sigma_{ij}^{(0)} - \nabla\sigma_{ij}^{(1)} \tag{1}$$

in which the stresses  $\sigma_{ij}^{(0)}$  and  $\sigma_{ij}^{(1)}$  are corresponding to strain  $\varepsilon_{ij}$  and strain gradient  $\nabla\varepsilon_{ij}$ , respectively as

$$\sigma_{ij}^{(0)} = \int_V C_{ijkl}\alpha_0(x, x', e_0a)\varepsilon'_{kl}(x')dx' \tag{2a}$$

$$\sigma_{ij}^{(1)} = l^2 \int_V C_{ijkl}\alpha_1(x, x', e_1a)\nabla\varepsilon'_{kl}(x')dx' \tag{2b}$$

in which  $C_{ijkl}$  are the elastic coefficients and  $e_0a$  and  $e_1a$  capture the nonlocal effects and  $l$  captures the strain gradient effects. When the nonlocal functions  $\alpha_0(x, x', e_0a)$  and  $\alpha_1(x, x', e_1a)$  satisfy the developed conditions by Eringen, the constitutive relation of nonlocal strain gradient theory has the following form

$$[1 - (e_1a)^2\nabla^2][1 - (e_0a)^2\nabla^2]\sigma_{ij} = C_{ijkl}[1 - (e_1a)^2\nabla^2]\varepsilon_{kl} - C_{ijkl}l^2[1 - (e_0a)^2\nabla^2]\nabla^2\varepsilon_{kl} \tag{3}$$

in which  $\nabla^2$  denotes the Laplacian operator. Considering  $e_1 = e_0 = e$ , the general constitutive relation in Eq. (3) becomes

$$[1 - (ea)^2\nabla^2]\sigma_{ij} = C_{ijkl}[1 - l^2\nabla^2]\varepsilon_{kl} \tag{4}$$

### 3. Porous nanoplate model with different porosity distributions

Assume a rectangular porous nanoplate with thickness  $h$  as illustrated in Figs. 1 and 2. Different types of porosity distribution have been considered: (1) uniform distribution; (2) non-uniform distribution 1 (symmetric); (3) non-uniform distribution 1 (asymmetric).

In the case of non-uniform distribution 1, the lowest values of elasticity moduli and mass density occur at the mid-plane of the nanoplate due to the largest size of nano-pores; while the

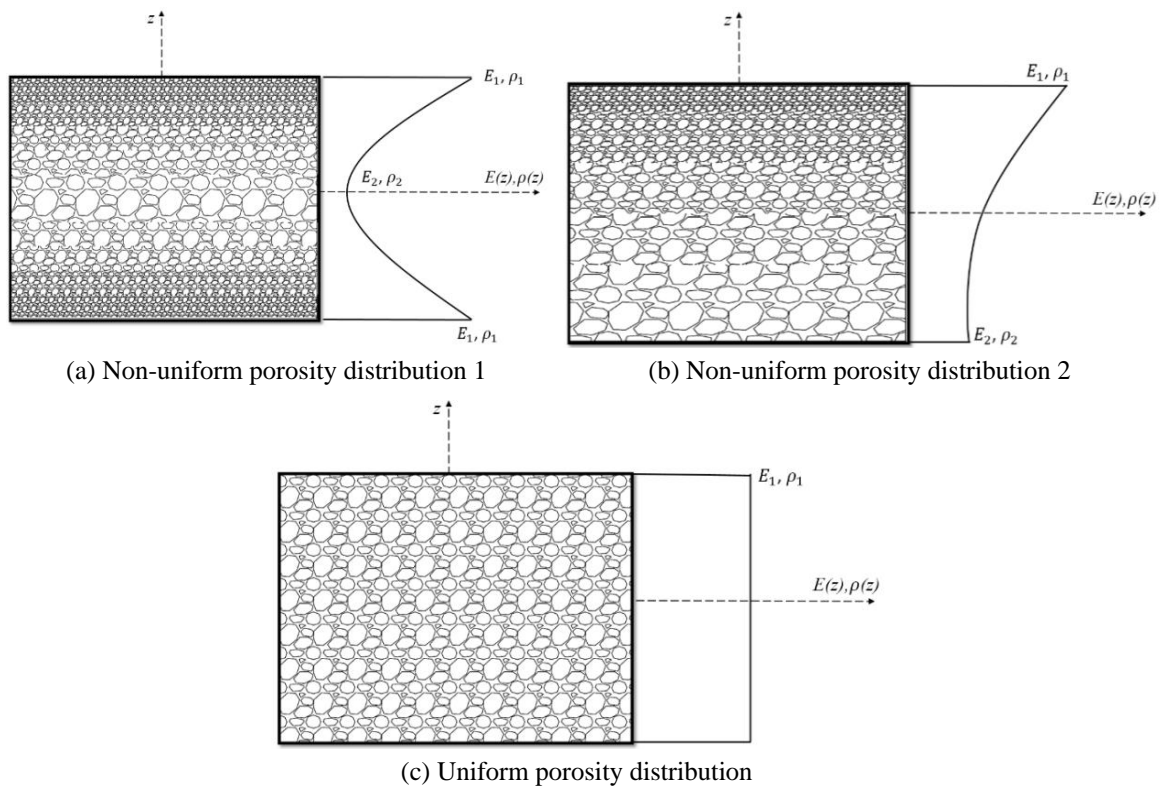


Fig. 1 Porosity distributions in the thickness direction

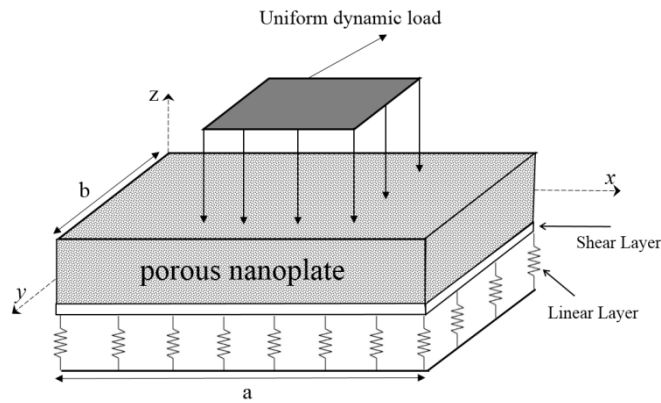


Fig. 2 Configuration of porous nanoplate under dynamic load

highest values of elasticity moduli and mass density occur at the top and bottom sides. In the case of non-uniform distribution 2, the elasticity moduli and mass density change gradually from their highest values at the top surface to a lowest value at bottom surface. The mechanical properties of a saturated porous nanoplate with different types of porosity distributions can be expressed by (Chen *et al.* 2016)

- Uniform porosity distribution

$$E = E_2(1 - e_0\chi) \tag{5a}$$

$$G = G_2(1 - e_0\chi) \tag{5b}$$

$$\rho = \rho_2\sqrt{(1 - e_0\chi)} \tag{5c}$$

- Non-uniform distribution 1

$$E(z) = E_2\left(1 - e_0 \cos\left(\frac{\pi z}{h}\right)\right) \tag{6a}$$

$$G(z) = G_2\left(1 - e_0 \cos\left(\frac{\pi z}{h}\right)\right) \tag{6b}$$

$$\rho(z) = \rho_2\left(1 - e_m \cos\left(\frac{\pi z}{h}\right)\right) \tag{6c}$$

- Non-uniform distribution 2

$$E(z) = E_2\left(1 - e_0 \cos\left(\frac{\pi z}{2h} + \frac{\pi}{4}\right)\right) \tag{7a}$$

$$G(z) = G_2\left(1 - e_0 \cos\left(\frac{\pi z}{2h} + \frac{\pi}{4}\right)\right) \tag{7b}$$

$$\rho(z) = \rho_2\left(1 - e_m \cos\left(\frac{\pi z}{2h} + \frac{\pi}{4}\right)\right) \tag{7c}$$

where  $E_2$ ,  $G_2$  and  $\rho_2$  are the maximum values of elasticity moduli, shear moduli and mass density;  $e_0$  and  $e_m$  are the coefficients of porosity and mass density, respectively defined by

$$e_0 = 1 - \frac{E_2}{E_1} = 1 - \frac{G_2}{G_1} \tag{8a}$$

$$e_m = 1 - \frac{\rho_2}{\rho_1} \tag{8b}$$

Also,  $e_m$  can be determined based on the typical mechanical properties of an open-cell metal foam as

$$\frac{E_2}{E_1} = \left(\frac{\rho_2}{\rho_1}\right)^2 \tag{9a}$$

$$e_m = 1 - \sqrt{1 - e_0} \quad (9b)$$

In the case of uniform porosity distribution, the material properties are constant through the thickness direction and they are only dependent on porosity coefficient  $e_0$ . Then, the coefficient  $\chi$  is expressed by

$$\chi = \frac{1}{e_0} - \frac{1}{e_0} \left( \frac{2}{\pi} \sqrt{1 - e_0} - \frac{2}{\pi} + 1 \right)^2 \quad (10)$$

Assuming four field variables, the displacement field of the nanoplate can be supposed as

$$u_1(x, y, z, t) = u(x, y, t) - (z - z^*) \frac{\partial w_b}{\partial x} - [f(z) - z^{**}] \frac{\partial w_s}{\partial x} \quad (11a)$$

$$u_2(x, y, z, t) = v(x, y, t) - (z - z^*) \frac{\partial w_b}{\partial y} - [f(z) - z^{**}] \frac{\partial w_s}{\partial y} \quad (11b)$$

$$u_3(x, y, z, t) = w(x, y, t) = w_b(x, y, t) + w_s(x, y, t) \quad (11c)$$

where

$$z^* = \frac{\int_{-h/2}^{h/2} E(z) z dz}{\int_{-h/2}^{h/2} E(z) dz}, \quad z^{**} = \frac{\int_{-h/2}^{h/2} E(z) f(z) dz}{\int_{-h/2}^{h/2} E(z) dz} \quad (12)$$

Also,  $u$  and  $v$  are in-plane displacements and  $w_b$  and  $w_s$  denote the bending and shear transverse displacement, respectively. Actually, this theory divides the total deflection of the plate into the bending and shear deflections. The shape function of transverse shear deformation is supposed as

$$f(z) = -\frac{z}{4} + \frac{5z^3}{3h^2} \quad (13)$$

It is now possible to obtain the strains based upon the present plate model as

$$\begin{aligned} \varepsilon_x &= \frac{\partial u}{\partial x} - (z - z^*) \frac{\partial^2 w_b}{\partial x^2} - [f(z) - z^{**}] \frac{\partial^2 w_s}{\partial x^2} \\ \varepsilon_y &= \frac{\partial v}{\partial y} - (z - z^*) \frac{\partial^2 w_b}{\partial y^2} - [f(z) - z^{**}] \frac{\partial^2 w_s}{\partial y^2} \\ \gamma_{xy} &= \frac{\partial u}{\partial y} + \frac{\partial v}{\partial x} - 2(z - z^*) \frac{\partial^2 w_b}{\partial x \partial y} - 2[f(z) - z^{**}] \frac{\partial^2 w_s}{\partial x \partial y} \\ \gamma_{yz} &= g(z) \frac{\partial w_s}{\partial y}, \quad \gamma_{xz} = g(z) \frac{\partial w_s}{\partial x} \end{aligned} \quad (14)$$

Now, Hamilton's principle can be written as

$$\int_0^t \delta(U - T - V) dt = 0 \tag{15}$$

here,  $U$  is strain energy,  $T$  is kinetic energy and  $V$  is work done by external forces. The first variation of the strain energy can be calculated as

$$\begin{aligned} \delta U = \int_V (\sigma_{xx} \delta \varepsilon_{xx} + \sigma_{xx}^{(1)} \delta \nabla \varepsilon_{xx} + \sigma_{yy} \delta \varepsilon_{yy} + \sigma_{yy}^{(1)} \delta \nabla \varepsilon_{yy} + \sigma_{xy} \delta \gamma_{xy} + \sigma_{xy}^{(1)} \delta \nabla \gamma_{xy} \\ + \sigma_{yz} \delta \gamma_{yz} + \sigma_{yz}^{(1)} \delta \nabla \gamma_{yz} + \sigma_{xz} \delta \gamma_{xz} + \sigma_{xz}^{(1)} \delta \nabla \gamma_{xz}) dV \end{aligned} \tag{16}$$

in which  $\sigma_{ij}$  are the components of the stress tensor and  $\varepsilon_{ij}$  are the components of the strain tensor.

$$\begin{aligned} \delta U = \int_0^a \int_0^b [N_{xx} [\frac{\partial \delta u}{\partial x} + \frac{\partial w}{\partial x} \frac{\partial \delta w}{\partial x}] - M_{xx}^b \frac{\partial^2 \delta w_b}{\partial x^2} - M_{xx}^s \frac{\partial^2 \delta w_s}{\partial x^2} + N_{yy} [\frac{\partial \delta v}{\partial y} + \frac{\partial w}{\partial y} \frac{\partial \delta w}{\partial y}] \\ - M_{yy}^b \frac{\partial^2 \delta w_b}{\partial y^2} - M_{yy}^s \frac{\partial^2 \delta w_s}{\partial y^2} + N_{xy} (\frac{\partial \delta u}{\partial y} + \frac{\partial \delta v}{\partial x} + \frac{\partial w}{\partial x} \frac{\partial \delta w}{\partial y} + \frac{\partial w}{\partial y} \frac{\partial \delta w}{\partial x}) - 2M_{xy}^b \frac{\partial^2 \delta w_b}{\partial x \partial y} \\ - 2M_{xy}^s \frac{\partial^2 \delta w_s}{\partial x \partial y} + Q_{yz} \frac{\partial \delta w_s}{\partial y} + Q_{xz} \frac{\partial \delta w_s}{\partial x}] dy dx \end{aligned} \tag{17}$$

in which

$$\begin{aligned} N_{xx} &= \int_{-h/2}^{h/2} (\sigma_{xx}^0 - \nabla \sigma_{xx}^{(1)}) dz = N_{xx}^{(0)} - \nabla N_{xx}^{(1)} \\ N_{xy} &= \int_{-h/2}^{h/2} (\sigma_{xy}^0 - \nabla \sigma_{xy}^{(1)}) dz = N_{xy}^{(0)} - \nabla N_{xy}^{(1)} \\ N_{yy} &= \int_{-h/2}^{h/2} (\sigma_{yy}^0 - \nabla \sigma_{yy}^{(1)}) dz = N_{yy}^{(0)} - \nabla N_{yy}^{(1)} \\ M_{xx}^b &= \int_{-h/2}^{h/2} z (\sigma_{xx}^0 - \nabla \sigma_{xx}^{(1)}) dz = M_{xx}^{b(0)} - \nabla M_{xx}^{b(1)} \\ M_{xx}^s &= \int_{-h/2}^{h/2} f (\sigma_{xx}^0 - \nabla \sigma_{xx}^{(1)}) dz = M_{xx}^{s(0)} - \nabla M_{xx}^{s(1)} \\ M_{yy}^b &= \int_{-h/2}^{h/2} z (\sigma_{yy}^0 - \nabla \sigma_{yy}^{(1)}) dz = M_{yy}^{b(0)} - \nabla M_{yy}^{b(1)} \\ M_{yy}^s &= \int_{-h/2}^{h/2} f (\sigma_{yy}^0 - \nabla \sigma_{yy}^{(1)}) dz = M_{yy}^{s(0)} - \nabla M_{yy}^{s(1)} \\ M_{xy}^b &= \int_{-h/2}^{h/2} z (\sigma_{xy}^0 - \nabla \sigma_{xy}^{(1)}) dz = M_{xy}^{b(0)} - \nabla M_{xy}^{b(1)} \\ M_{xy}^s &= \int_{-h/2}^{h/2} f (\sigma_{xy}^0 - \nabla \sigma_{xy}^{(1)}) dz = M_{xy}^{s(0)} - \nabla M_{xy}^{s(1)} \\ Q_{xz} &= \int_{-h/2}^{h/2} g (\sigma_{xz}^0 - \nabla \sigma_{xz}^{(1)}) dz = Q_{xz}^{(0)} - \nabla Q_{xz}^{(1)} \\ Q_{yz} &= \int_{-h/2}^{h/2} g (\sigma_{yz}^0 - \nabla \sigma_{yz}^{(1)}) dz = Q_{yz}^{(0)} - \nabla Q_{yz}^{(1)} \end{aligned} \tag{18a}$$

where

$$\begin{aligned}
N_{ij}^{(0)} &= \int_{-h/2}^{h/2} (\sigma_{ij}^{(0)}) dz, & N_{ij}^{(1)} &= \int_{-h/2}^{h/2} (\sigma_{ij}^{(1)}) dz \\
M_{ij}^{b(0)} &= \int_{-h/2}^{h/2} z(\sigma_{ij}^{b(0)}) dz, & M_{ij}^{b(1)} &= \int_{-h/2}^{h/2} z(\sigma_{ij}^{b(1)}) dz \\
M_{ij}^{s(0)} &= \int_{-h/2}^{h/2} f(\sigma_{ij}^{s(0)}) dz, & M_{ij}^{s(1)} &= \int_{-h/2}^{h/2} f(\sigma_{ij}^{s(1)}) dz \\
Q_{xz}^{(0)} &= \int_{-h/2}^{h/2} g(\sigma_{xz}^{i(0)}) dz, & Q_{xz}^{(1)} &= \int_{-h/2}^{h/2} g(\sigma_{xz}^{i(1)}) dz \\
Q_{yz}^{(0)} &= \int_{-h/2}^{h/2} g(\sigma_{yz}^{i(0)}) dz, & Q_{yz}^{(1)} &= \int_{-h/2}^{h/2} g(\sigma_{yz}^{i(1)}) dz
\end{aligned} \tag{18b}$$

in which ( $ij = xx, xy, yy$ ). The first variation of the work done by applied forces can be written as

$$\begin{aligned}
\delta V &= \int_0^a \int_0^b (N_x^0 \frac{\partial(w_b + w_s)}{\partial x} \frac{\partial \delta(w_b + w_s)}{\partial x} + N_y^0 \frac{\partial(w_b + w_s)}{\partial y} \frac{\partial \delta(w_b + w_s)}{\partial y} \\
&\quad + 2\delta N_{xy}^0 \frac{\partial(w_b + w_s)}{\partial x} \frac{\partial(w_b + w_s)}{\partial y} - (k_w - q_{dynamic})(w_b + w_s)\delta(w_b + w_s) \\
&\quad + k_p (\frac{\partial(w_b + w_s)}{\partial x} \frac{\partial \delta(w_b + w_s)}{\partial x} + \frac{\partial(w_b + w_s)}{\partial y} \frac{\partial \delta(w_b + w_s)}{\partial y})) dy dx
\end{aligned} \tag{19}$$

where  $N_x^0, N_y^0, N_{xy}^0$  are in-plane applied loads;  $k_w$  and  $k_p$  are Winkler and Pasternak constants. Also,  $q_{dynamic}$  is the transverse force due to applied dynamic load. The first variation of the kinetic energy can be written in the following form

$$\begin{aligned}
\delta K &= \int_0^a \int_0^b [I_0 (\frac{\partial u}{\partial t} \frac{\partial \delta u}{\partial t} + \frac{\partial v}{\partial t} \frac{\partial \delta v}{\partial t} + \frac{\partial(w_b + w_s)}{\partial t} \frac{\partial \delta(w_b + w_s)}{\partial t}) - I_1 (\frac{\partial u}{\partial t} \frac{\partial \delta w_b}{\partial x \partial t} + \frac{\partial w_b}{\partial x \partial t} \frac{\partial \delta u}{\partial t} + \frac{\partial v}{\partial t} \frac{\partial \delta w_b}{\partial y \partial t} \\
&\quad + \frac{\partial w_b}{\partial y \partial t} \frac{\partial \delta v}{\partial t}) - I_2 (\frac{\partial u}{\partial t} \frac{\partial \delta w_s}{\partial x \partial t} + \frac{\partial w_s}{\partial x \partial t} \frac{\partial \delta u}{\partial t} + \frac{\partial v}{\partial t} \frac{\partial \delta w_s}{\partial y \partial t} + \frac{\partial w_s}{\partial y \partial t} \frac{\partial \delta v}{\partial t}) + I_3 (\frac{\partial w_b}{\partial x \partial t} \frac{\partial \delta w_b}{\partial x \partial t} + \frac{\partial w_b}{\partial y \partial t} \frac{\partial \delta w_b}{\partial y \partial t}) \\
&\quad + I_4 (\frac{\partial w_s}{\partial x \partial t} \frac{\partial \delta w_s}{\partial x \partial t} + \frac{\partial w_s}{\partial y \partial t} \frac{\partial \delta w_s}{\partial y \partial t}) + I_5 (\frac{\partial w_b}{\partial x \partial t} \frac{\partial \delta w_s}{\partial x \partial t} + \frac{\partial w_s}{\partial x \partial t} \frac{\partial \delta w_b}{\partial x \partial t} + \frac{\partial w_b}{\partial y \partial t} \frac{\partial \delta w_s}{\partial y \partial t} + \frac{\partial w_s}{\partial y \partial t} \frac{\partial \delta w_b}{\partial y \partial t})] dy dx
\end{aligned} \tag{20}$$

in which

$$(I_0, I_1, I_2, I_3, I_4, I_5) = \int_{-h/2}^{h/2} (1, z - z^*, (z - z^*)^2, f - z^{**}, (z - z^*)(f - z^{**}), (f - z^{**})^2) \rho(z) dz \tag{21}$$

By inserting Eqs. (17)-(20) into Eq. (15) and setting the coefficients of  $\delta u$ ,  $\delta v$ ,  $\delta w_b$  and  $\delta w_s$  to zero, the following Euler–Lagrange equations can be obtained.

$$\frac{\partial N_x}{\partial x} + \frac{\partial N_{xy}}{\partial y} = I_0 \frac{\partial^2 u}{\partial t^2} - I_1 \frac{\partial^3 w_b}{\partial x \partial t^2} - I_3 \frac{\partial^3 w_s}{\partial x \partial t^2} \tag{22a}$$

$$\frac{\partial N_{xy}}{\partial x} + \frac{\partial N_y}{\partial y} = I_0 \frac{\partial^2 v}{\partial t^2} - I_1 \frac{\partial^3 w_b}{\partial y \partial t^2} - I_3 \frac{\partial^3 w_s}{\partial y \partial t^2} \tag{22b}$$

$$\begin{aligned} & \frac{\partial^2 M_x^b}{\partial x^2} + 2 \frac{\partial^2 M_{xy}^b}{\partial x \partial y} + \frac{\partial^2 M_y^b}{\partial y^2} - k_w(w_b + w_s) + k_p \nabla^2(w_b + w_s) - q_{dynamic} \\ & = +I_0 \frac{\partial^2(w_b + w_s)}{\partial t^2} + I_1 \left( \frac{\partial^3 u}{\partial x \partial t^2} + \frac{\partial^3 v}{\partial y \partial t^2} \right) - I_2 \nabla^2 \left( \frac{\partial^2 w_b}{\partial t^2} \right) - I_4 \nabla^2 \left( \frac{\partial^2 w_s}{\partial t^2} \right) \end{aligned} \tag{22c}$$

$$\begin{aligned} & \frac{\partial^2 M_x^s}{\partial x^2} + 2 \frac{\partial^2 M_{xy}^s}{\partial x \partial y} + \frac{\partial^2 M_y^s}{\partial y^2} + \frac{\partial Q_{xz}}{\partial x} + \frac{\partial Q_{yz}}{\partial y} - k_w(w_b + w_s) - q_{dynamic} \\ & + k_p \nabla^2(w_b + w_s) = I_0 \frac{\partial^2(w_b + w_s)}{\partial t^2} + I_3 \left( \frac{\partial^3 u}{\partial x \partial t^2} + \frac{\partial^3 v}{\partial y \partial t^2} \right) - I_4 \nabla^2 \left( \frac{\partial^2 w_b}{\partial t^2} \right) - I_5 \nabla^2 \left( \frac{\partial^2 w_s}{\partial t^2} \right) \end{aligned} \tag{22d}$$

The classical and non-classical boundary conditions can be obtained in the derivation process when using the integrations by parts. Thus, we obtain classical boundary conditions at  $x = 0$  or  $a$  and  $y = 0$  or  $b$  as

$$\begin{aligned} & \text{Specify } w_b \text{ or } \left( \frac{\partial M_{xx}^b}{\partial x} + \frac{\partial M_{xy}^b}{\partial y} \right) n_x + \left( \frac{\partial M_{yy}^b}{\partial y} + \frac{\partial M_{xy}^b}{\partial x} \right) n_y = 0 \\ & \text{Specify } w_s \text{ or } \left( \frac{\partial M_{xx}^s}{\partial x} + \frac{\partial M_{xy}^s}{\partial y} + Q_{xz} \right) n_x + \left( \frac{\partial M_{yy}^s}{\partial y} + \frac{\partial M_{xy}^s}{\partial x} + Q_{yz} \right) n_y = 0 \tag{23a} \\ & \text{Specify } \frac{\partial w_b}{\partial n} \text{ or } M_{xx}^b n_x^2 + n_x n_y M_{xy}^b + M_{yy}^b n_y^2 = 0 \end{aligned}$$

where  $\frac{\partial()}{\partial n} = n_x \frac{\partial()}{\partial x} + n_y \frac{\partial()}{\partial y}$ ;  $n_x$  and  $n_y$  are the  $x$  and  $y$ -components of the unit normal vector on the nanoplate boundaries, respectively and the non-classical boundary conditions are

$$\begin{aligned} & \text{Specify } \frac{\partial^2 w_b}{\partial x^2} \text{ or } M_{xx}^{b(1)} = 0 & \text{Specify } \frac{\partial^2 w_s}{\partial x^2} \text{ or } M_{xx}^{s(1)} = 0 \\ & \text{Specify } \frac{\partial^2 w_b}{\partial y^2} \text{ or } M_{yy}^{b(1)} = 0 & \text{Specify } \frac{\partial^2 w_s}{\partial y^2} \text{ or } M_{yy}^{s(1)} = 0 \end{aligned} \tag{23b}$$

Based on the NSGT, the constitutive relations of presented higher order nanoplate can be stated as

$$(1 - \mu \nabla^2) \begin{Bmatrix} \sigma_x \\ \sigma_y \\ \sigma_{xy} \\ \sigma_{yz} \\ \sigma_{xz} \end{Bmatrix} = \frac{E(z)}{1 - \nu^2} (1 - \lambda \nabla^2) \begin{pmatrix} 1 & \nu & 0 & 0 & 0 \\ \nu & 1 & 0 & 0 & 0 \\ 0 & 0 & (1-\nu)/2 & 0 & 0 \\ 0 & 0 & 0 & (1-\nu)/2 & 0 \\ 0 & 0 & 0 & 0 & (1-\nu)/2 \end{pmatrix} \begin{Bmatrix} \epsilon_x \\ \epsilon_y \\ \gamma_{xy} \\ \gamma_{yz} \\ \gamma_{xz} \end{Bmatrix} \tag{24}$$

Integrating Eq. (24) over the plate thickness, one can obtain the force-strain and the moment-strain of the nonlocal refined plates can be obtained as follows

$$(1 - \mu \nabla^2) \begin{Bmatrix} N_x \\ N_y \\ N_{xy} \end{Bmatrix} = A(1 - \lambda \nabla^2) \begin{pmatrix} 1 & \nu & 0 \\ \nu & 1 & 0 \\ 0 & 0 & (1-\nu)/2 \end{pmatrix} \begin{Bmatrix} \frac{\partial u}{\partial x} \\ \frac{\partial v}{\partial y} \\ \frac{\partial u}{\partial y} + \frac{\partial v}{\partial x} \end{Bmatrix} \quad (25)$$

$$(1 - \mu \nabla^2) \begin{Bmatrix} M_x^b \\ M_y^b \\ M_{xy}^b \end{Bmatrix} = D(1 - \lambda \nabla^2) \begin{pmatrix} 1 & \nu & 0 \\ \nu & 1 & 0 \\ 0 & 0 & (1-\nu)/2 \end{pmatrix} \begin{Bmatrix} -\frac{\partial^2 w_b}{\partial x^2} \\ -\frac{\partial^2 w_b}{\partial y^2} \\ -2\frac{\partial^2 w_b}{\partial x \partial y} \end{Bmatrix} + E(1 - \lambda \nabla^2) \begin{pmatrix} 1 & \nu & 0 \\ \nu & 1 & 0 \\ 0 & 0 & (1-\nu)/2 \end{pmatrix} \begin{Bmatrix} \frac{\partial^2 w_s}{\partial x^2} \\ \frac{\partial^2 w_s}{\partial y^2} \\ -2\frac{\partial^2 w_s}{\partial x \partial y} \end{Bmatrix} \quad (26)$$

$$(1 - \mu \nabla^2) \begin{Bmatrix} M_x^s \\ M_y^s \\ M_{xy}^s \end{Bmatrix} = E(1 - \lambda \nabla^2) \begin{pmatrix} 1 & \nu & 0 \\ \nu & 1 & 0 \\ 0 & 0 & (1-\nu)/2 \end{pmatrix} \begin{Bmatrix} -\frac{\partial^2 w_b}{\partial x^2} \\ -\frac{\partial^2 w_b}{\partial y^2} \\ -2\frac{\partial^2 w_b}{\partial x \partial y} \end{Bmatrix} + F(1 - \lambda \nabla^2) \begin{pmatrix} 1 & \nu & 0 \\ \nu & 1 & 0 \\ 0 & 0 & (1-\nu)/2 \end{pmatrix} \begin{Bmatrix} \frac{\partial^2 w_s}{\partial x^2} \\ \frac{\partial^2 w_s}{\partial y^2} \\ -2\frac{\partial^2 w_s}{\partial x \partial y} \end{Bmatrix} \quad (27)$$

$$(1 - \mu \nabla^2) \begin{Bmatrix} Q_x \\ Q_y \end{Bmatrix} = A_{44}(1 - \lambda \nabla^2) \begin{pmatrix} 1 & 0 \\ 0 & 1 \end{pmatrix} \begin{Bmatrix} \frac{\partial w_s}{\partial x} \\ \frac{\partial w_s}{\partial y} \end{Bmatrix} \quad (28)$$

in which

$$A = \int_{-h/2}^{h/2} \frac{E(z)}{1-\nu^2} dz, \quad D = \int_{-h/2}^{h/2} \frac{E(z)(z-z^*)^2}{1-\nu^2} dz, \quad E = \int_{-h/2}^{h/2} \frac{E(z)(z-z^*)(f-z^{**})}{1-\nu^2} dz \quad (29)$$

$$F = \int_{-h/2}^{h/2} \frac{E(z)(f-z^{**})^2}{1-\nu^2} dz, \quad A_{44} = \int_{-h/2}^{h/2} \frac{E(z)}{2(1+\nu)} g^2 dz$$

The governing equations in terms of the displacements for a NSGT refined four-variable nanoplate can be derived by substituting Eqs. (25)-(28), into Eq. (22) as follows

$$\begin{aligned} & -D(1 - \lambda \nabla^2) \left( \frac{\partial^4 w_b}{\partial x^4} + 2 \frac{\partial^4 w_b}{\partial x^2 \partial y^2} + \frac{\partial^4 w_b}{\partial y^4} \right) - E(1 - \lambda \nabla^2) \left( \frac{\partial^4 w_s}{\partial x^4} + 2 \frac{\partial^4 w_s}{\partial x^2 \partial y^2} + \frac{\partial^4 w_s}{\partial y^4} \right) \\ & + (1 - \mu \nabla^2) \left( -I_0 \frac{\partial^2 (w_b + w_s)}{\partial t^2} + I_2 \nabla^2 \left( \frac{\partial^2 w_b}{\partial t^2} \right) + I_4 \nabla^2 \left( \frac{\partial^2 w_s}{\partial t^2} \right) \right) \\ & - k_w (w_b + w_s) + k_p \nabla^2 (w_b + w_s) = q_{dynamic} - \mu \frac{\partial^2 q_{dynamic}}{\partial x^2} \end{aligned} \quad (30)$$

$$\begin{aligned}
 & -E(1-\lambda\nabla^2)\left(\frac{\partial^4 w_b}{\partial x^4} + 2\frac{\partial^4 w_b}{\partial x^2\partial y^2} + \frac{\partial^4 w_b}{\partial y^4}\right) - F(1-\lambda\nabla^2)\left(\frac{\partial^4 w_s}{\partial x^4} + 2\frac{\partial^4 w_s}{\partial x^2\partial y^2} + \frac{\partial^4 w_s}{\partial y^4}\right) \\
 & + A_{44}(1-\lambda\nabla^2)\left(\frac{\partial^2 w_s}{\partial x^2} + \frac{\partial^2 w_s}{\partial y^2}\right) + (1-\mu\nabla^2)\left(-I_0\frac{\partial^2(w_b+w_s)}{\partial t^2}\right) \\
 & + I_4\nabla^2\left(\frac{\partial^2 w_b}{\partial t^2}\right) + I_5\nabla^2\left(\frac{\partial^2 w_s}{\partial t^2}\right) - k_w(w_b+w_s) + k_p\nabla^2(w_b+w_s) = q_{dynamic} - \mu\frac{\partial^2 q_{dynamic}}{\partial x^2}
 \end{aligned} \tag{31}$$

#### 4. Solution procedure

In this section, Galerkin’s method is implemented to solve the governing equations of nonlocal strain gradient based double-layered nanoplates. Thus, the displacement field can be calculated as

$$w_b = \sum_{m=1}^{\infty} \sum_{n=1}^{\infty} W_{bmn} X_m(x) Y_n(y) e^{i\omega_s t} \tag{32}$$

$$w_s = \sum_{m=1}^{\infty} \sum_{n=1}^{\infty} W_{smn} X_m(x) Y_n(y) e^{i\omega_s t} \tag{33}$$

where ( $W_{bmn}, W_{smn}$ ) are the unknown coefficients and the functions  $X_m$  and  $Y_n$  satisfy the boundary conditions. The classical and non-classical boundary condition based on the present plate model are

$$\begin{aligned}
 & w_b = w_s = 0, \\
 & \frac{\partial^2 w_b}{\partial x^2} = \frac{\partial^2 w_s}{\partial x^2} = \frac{\partial^2 w_b}{\partial y^2} = \frac{\partial^2 w_s}{\partial y^2} = 0 \\
 & \frac{\partial^4 w_b}{\partial x^4} = \frac{\partial^4 w_s}{\partial x^4} = \frac{\partial^4 w_b}{\partial y^4} = \frac{\partial^4 w_s}{\partial y^4} = 0
 \end{aligned} \tag{34}$$

By substituting Eqs. (32) and (33) into Eqs. (30) and (31), and using the Galerkin’s method, one obtains

$$\{[K] + \omega_{ex}^2[M]\} \begin{Bmatrix} W_{bmn} \\ W_{smn} \end{Bmatrix} = \begin{Bmatrix} Q_{dynamic} \\ Q_{dynamic} \end{Bmatrix} \tag{35}$$

in which  $\omega_{ex}$  is the excitation frequency and the components of mass and stiffness matrices are presented in Appendix.

$$K_w = \frac{k_w a^4}{D_2}, K_0 = \frac{k_0 a^4}{D_2}, K_p = \frac{k_p a^2}{D_2}, D_1 = \frac{E_2 h^3}{12(1-\nu^2)}, \mu = \frac{ea}{a}, \lambda = \frac{l}{a} \tag{36}$$

Finally, setting the coefficient matrix to zero gives the natural frequencies. The function  $X_m$  for simply-supported boundary conditions is defined by

$$X_m(x) = \sin(\lambda_m x)$$

$$\lambda_m = \frac{m\pi}{a} \quad (37)$$

The function  $Y_n$  can be obtained by replacing  $x$ ,  $m$  and  $a$ , respectively by  $y$ ,  $n$  and  $b$ . It is supposed that the dynamic load is distributed uniformly acting harmonically along a straight line leading to forced vibration and is expressed by the following form

$$q_{dynamic} = \sum_{n=1}^{\infty} Q_n \sin\left[\frac{m\pi}{a} x\right] \sin\left[\frac{n\pi}{b} y\right] \sin \omega t \quad (38)$$

$$Q_n = \frac{4q_0}{mn} \int_{x_0-0.5a_0}^{x_0+0.5a_0} \int_{y_0-0.5b_0}^{y_0+0.5b_0} \sin\left[\frac{m\pi}{a} x\right] \sin\left[\frac{n\pi}{b} y\right] q(x) dx$$

$$= \frac{16q_0}{mn\pi^2} \sin\left[\frac{m\pi}{a} x_0\right] \sin\left[\frac{m\pi a_0}{2a}\right] \sin\left[\frac{n\pi}{b} y_0\right] \sin\left[\frac{n\pi b_0}{2b}\right] \quad (39)$$

in which  $Q_n$  are the Fourier coefficients and  $q(x) = q_0$  is the uniform load density;  $x_0$  and  $y_0$  are the centroid coordinate. Solution of Eq. (35) gives the bending ( $W_{bn}$ ) and shear ( $W_{sn}$ ) components of transverse displacement. The dynamic deflection of a higher order refined nanoplate can be obtained by  $W = W_{bn} + W_{sn}$ . The dimensionless excitation frequency and forced vibration amplitude are defined as

$$\Omega = \omega_{ex} a \sqrt{\frac{\rho_2}{E_2}}, \quad \bar{W}_{uniform} = W \frac{10E_2 h^3}{a^4 q_0} \quad (40)$$

## 5. Numerical results and discussions

In this section, results are presented for forced vibration study of size-dependent porous nanoplates modeled via a 4-unknown plate model and NSGT. The nanoplate is subjected to a uniform dynamic load shown in Fig. 3. First of all, the frequency response of the present study is validated with those of classical nanoplate model with graded material properties obtained by Natarajan *et al.* (2012) through finite element approach. These results are tabulated in Table 1 for fully simply-supported edge conditions and a good agreement is observed. In the present study, the material properties of metal foam nanoplate are considered as

- $E_2 = 200$  GPa,  $\rho_2 = 7850$  kg/m<sup>3</sup>,  $\nu = 0.33$ ,

Fig. 4 shows the influence of strain gradient parameter ( $\lambda$ ) and nonlocality parameter ( $\mu$ ) on the dynamic deflection and resonance frequencies of porous nanoplates versus excitation frequency at  $a/h = 10$ ,  $e_0 = 0.5$  and  $K_w = K_p = 0$ . It is evident that dynamic deflection of the nanoplate is prominently affected by the magnitude of excitation frequency of dynamic load. In fact, dynamic deflection increases smoothly with the increase of excitation frequency. At a certain value of excitation frequency, a notable increase in deflection of nanoplate is observed. The reason is that the excitation frequency of dynamic load coincides with the natural frequency of the nanoplate leading to the resonance phenomena. Resonance frequencies of a macro scale plate are obtained by setting  $\mu = \lambda = 0$ . Also, setting  $\lambda = 0$  results in the analysis of a nanoplate via nonlocal elasticity

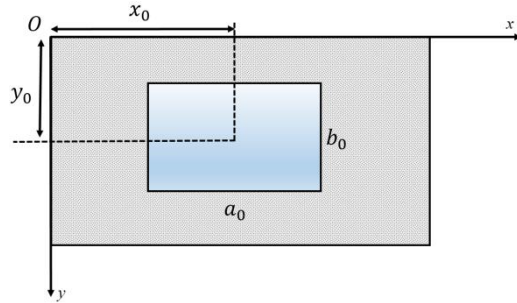


Fig. 3 The top view of nanoplate and location of dynamic load

Table 1 Comparison of non-dimensional fundamental natural frequency of nanoplates with simply-supported boundary conditions

$a/h$	$\mu$	$a/b = 1$		$a/b = 2$	
		Natarajan <i>et al.</i> (2012)	Present	Natarajan <i>et al.</i> (2012)	Present
10	0	0.0441	0.043823	0.1055	0.104329
	1	0.0403	0.04007	0.0863	0.085493
	2	0.0374	0.037141	0.0748	0.074174
	4	0.0330	0.032806	0.0612	0.060673
20	0	0.0113	0.011256	0.0279	0.027756
	1	0.0103	0.010288	0.0229	0.022722
	2	0.0096	0.009534	0.0198	0.019704
	4	0.0085	0.008418	0.0162	0.016110

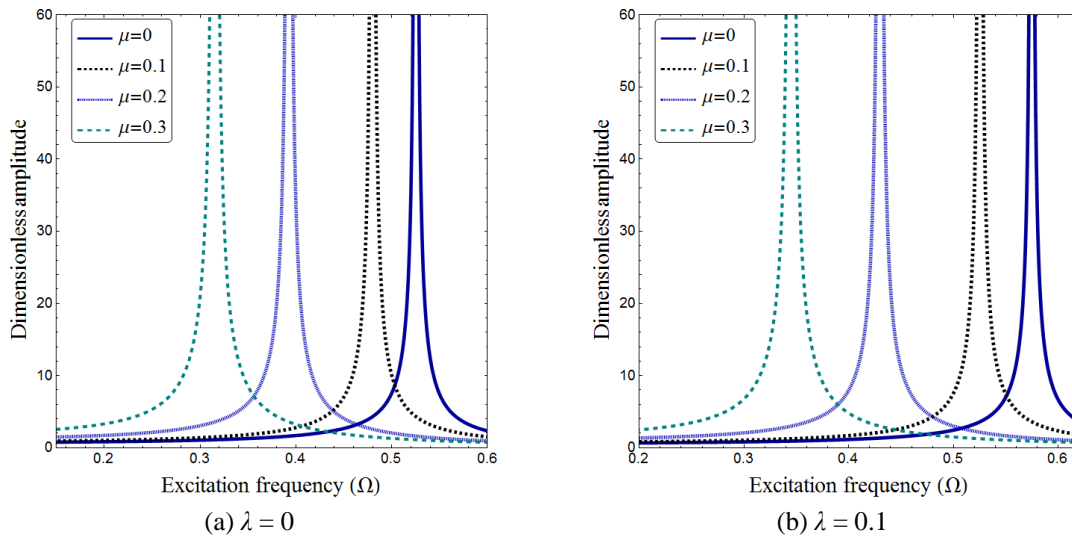
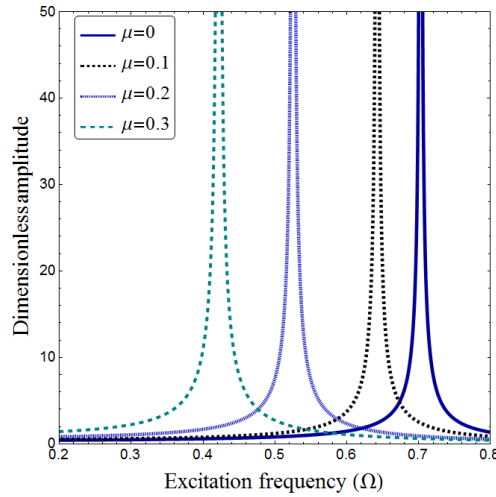


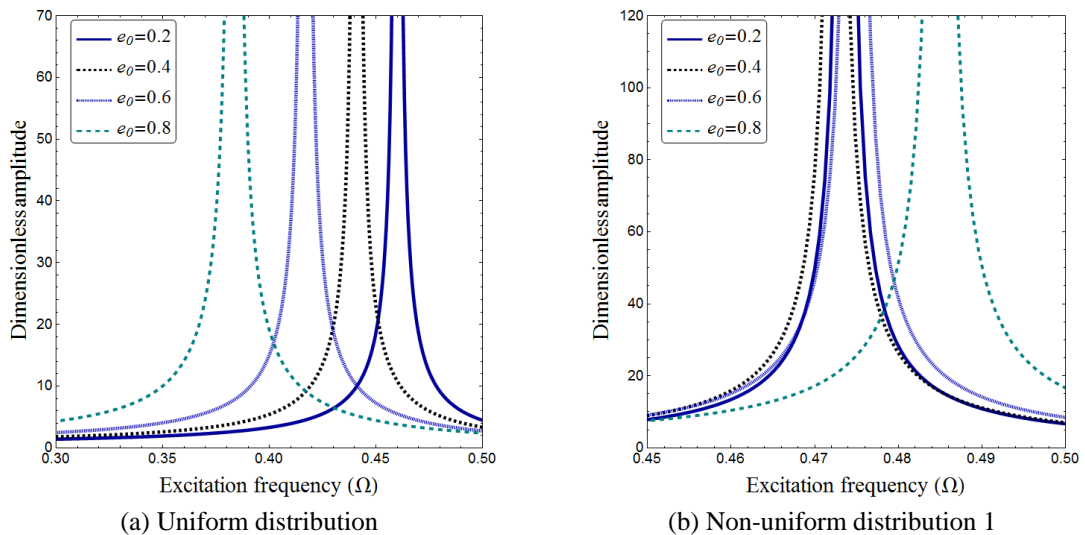
Fig. 4 Dimensionless amplitude of the nanoplate versus excitation frequency for different nonlocal and strain gradient parameters ( $a/h = 10, K_w = 0, K_p = 0, e_0 = 0.5$ )



(c)  $\lambda = 0.2$

Fig. 4 Continued

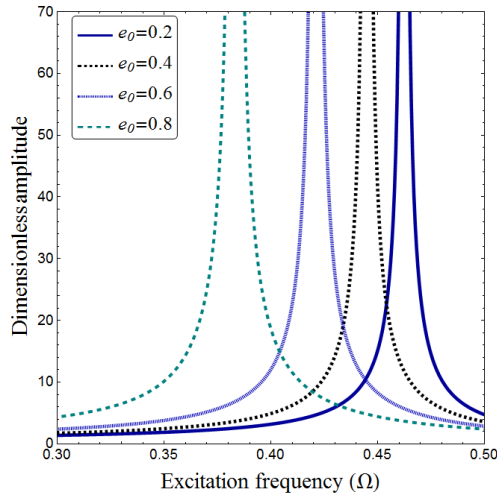
theory neglecting strain gradient effects. One can see that nonlocal coefficient provides a stiffness reduction mechanism leading to smaller resonance frequencies and larger dynamic deflections for all values of strain gradient coefficient. But, a different mechanism is introduced by strain gradient coefficient. Therefore, increasing in strain gradient coefficient results in larger resonance frequencies. The competition between these two scale parameters clarifies the importance of presented nonlocal strain gradient theory. For example, obtained frequencies are respectively smaller and larger than that of classical elasticity theory at  $\lambda < \mu$  and  $\lambda > \mu$ . Such important facts must be considered in analysis of nanoplates.



(a) Uniform distribution

(b) Non-uniform distribution 1

Fig. 5 Dimensionless amplitude of the nanoplate versus excitation frequency for different porosity distributions ( $a/h = 10, K_w = 0, K_p = 0, \mu = 0.2, \lambda = 0.1$ )



(c) Non-uniform distribution 2

Fig. 5 Continued

Porosity effect on the dynamic deflection and resonance frequencies of porous nanoplates with respect to excitation frequency is presented in Fig. 5 at  $\mu = 0.2$ ,  $K_w = 0$  and  $K_p = 0$ . An increase in porosity coefficient yields larger resonance frequencies for nanoplates with porosity distribution 1 while lower resonance frequencies for nanoplates with uniform porosities and distribution 2. Obtained results show that as the porosity coefficient increases, the nanoplate with porosity distribution 1 has the highest resonance frequency whereas the results of the nanoplates with uniform porosity distribution and graded porosity distribution 2 are quite close. This indicates that the nanoplate with symmetrically distributed porosity can achieve the highest plate stiffness

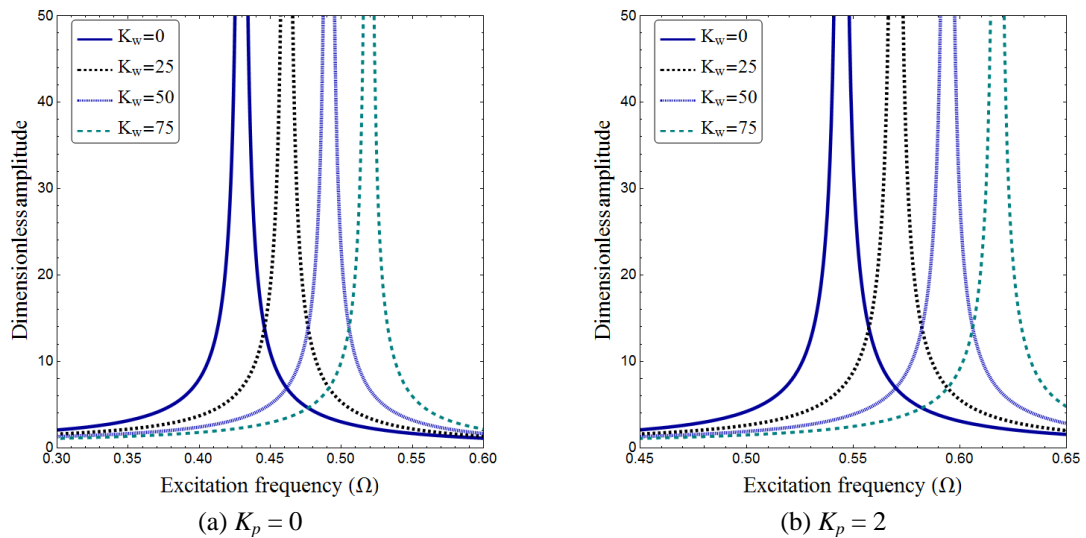


Fig. 6 Dimensionless amplitude of the nanoplate versus excitation frequency for various foundation constants and uniform porosity distribution ( $a/h = 10$ ,  $\mu = 0.2$ ,  $e_0 = 0.5$ )

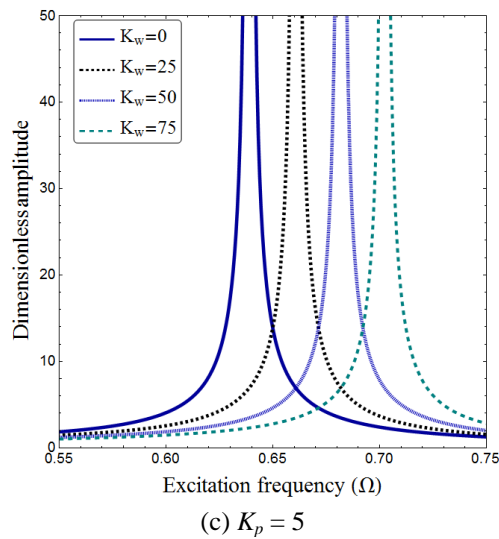


Fig. 6 Continued

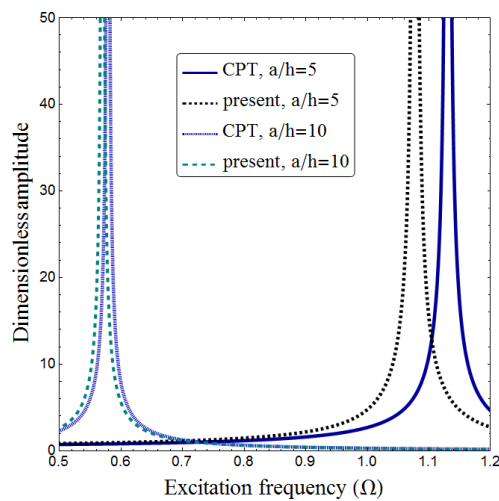


Fig. 7 Dimensionless amplitude of the nanoplate versus excitation frequency according to the classical and present plate theories ( $\mu = 0.2, \lambda = 0.1, K_w = 25, K_p = 5, e_0 = 0.5$ )

hence the best mechanical performance. Therefore, porosity distribution has a major role on vibration behavior and should be considered in dynamic analysis of nanoplates.

In Fig. 6, the effects of Winkler-Pasternak constants on dynamic deflection and resonance frequencies of porous nanoplates with uniform porosities are demonstrated when  $a/h = 10, e_0 = 0.5, \mu = 0.2$  and  $\lambda = 0.1$ . One can see that resonance frequencies are dependent on the magnitudes of both Winkler and Pasternak coefficients. Increasing in Winkler and Pasternak coefficients yields enhancement of the bending rigidity and resonance frequency of system. Since Pasternak layer has a continuous interaction with nanoplates, its effect on resonance frequencies is more sensible compared with Winkler layer.

A comparison between the dynamic deflection and resonance frequencies of the nanoplate based on classical and higher order refined plate theory is presented in Fig. 7 at  $e_0 = 0.5$ ,  $K_w = 25$ ,  $K_p = 5$ . It is well-known that classical plate theory is unable to consider shear deformation effects. Thus, dynamic deflections in pre-resonance region obtained based on classical plate model are smaller than that of refined plate theory. In other words, classical plate theory gives larger resonance frequencies than refined theory. Therefore, analysis of forced vibration of nanoplates based on higher order refined theories is more reliable than classical plate theory.

A study on the effects of dynamic load area ( $a_0/a$ ,  $b_0/b$ ) and location ( $x_0/a$ ) on non-dimensional deflection of porous nanoplate with respect to excitation frequency is performed in Figs. 8 and 9,

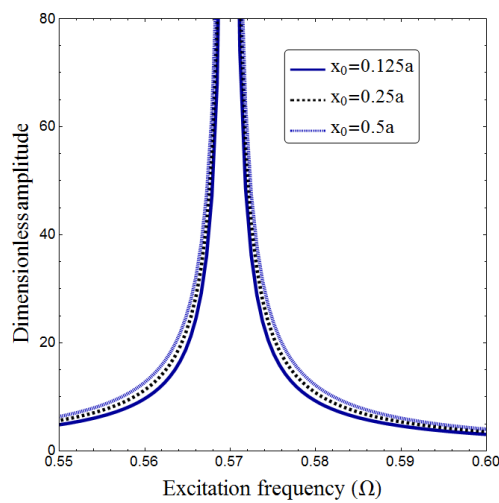


Fig. 8 Dimensionless amplitude of the nanoplate versus excitation frequency according to various location of dynamic load ( $\mu = 0.2$ ,  $\lambda = 0.1$ ,  $K_w = 25$ ,  $K_p = 5$ ,  $e_0 = 0.5$ )

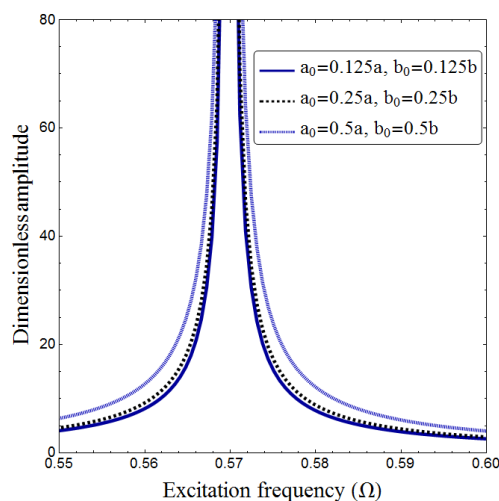


Fig. 9 Dimensionless amplitude of the nanoplate versus excitation frequency according to various area of dynamic load ( $\mu = 0.2$ ,  $\lambda = 0.1$ ,  $K_w = 25$ ,  $K_p = 5$ ,  $e_0 = 0.5$ )

respectively. In these figures, it is considered that  $a/h = 10$ ,  $K_w = 25$ ,  $K_p = 5$ ,  $\mu = 0.2$ ,  $\lambda = 0.1$  and  $e_0 = 0.5$ . It can be observed that as the transverse load moves away from the boundaries, the dynamic deflection enlarges. In fact, the region of frequency– response curves of the nanoplate becomes wider. Similarly, increasing the area of applied dynamic load on the nanoplate leads to larger deflections. But, the area and location of dynamic load have no effect on the magnitude of resonance frequency. Because the resonance frequency or natural frequency of system is an inherent property of that system. So, it is not affected by the geometrical parameters of external load.

In Figs. 10 and 11, the first mode shape of the nanoplate under uniform dynamic load for various porosity coefficients and distributions is shown at  $\Omega = 0.1$ ,  $\mu = 0.2$ ,  $\lambda = 0.1$ ,  $K_w = 25$ ,  $K_p = 5$ .

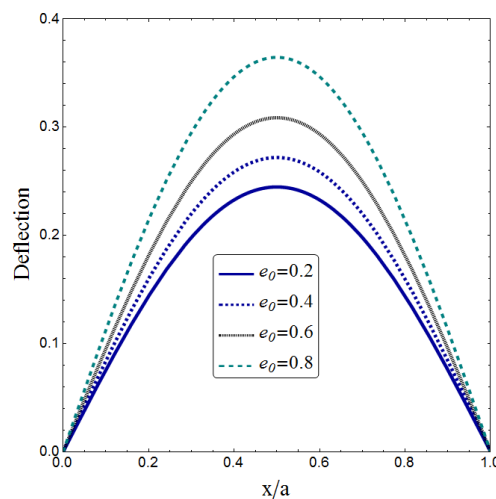


Fig. 10 Mode shape of the nanoplate for different uniform porosity coefficients ( $a/h = 10$ ,  $y = 0.5b$ ,  $\Omega = 0.1$ ,  $K_w = 25$ ,  $K_p = 5$ ,  $a_0/a = 0.125$ ,  $b_0/b = 0.125$ ,  $x_0 = 0.5a$ )

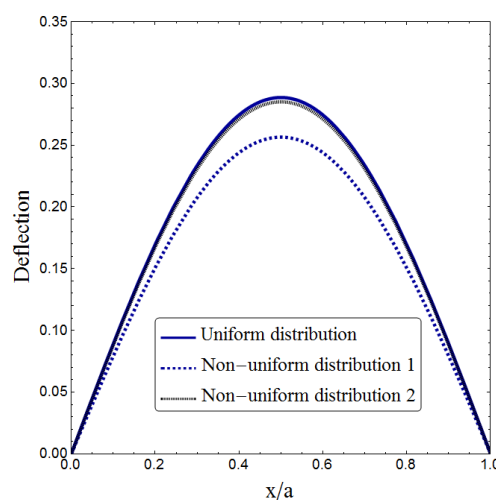


Fig. 11 Mode shape of the nanoplate for different porosity distributions ( $a/h = 10$ ,  $y = 0.5b$ ,  $\Omega = 0.1$ ,  $K_w = 25$ ,  $K_p = 5$ ,  $e_0 = 0.5$ ,  $a_0/a = 0.125$ ,  $b_0/b = 0.125$ ,  $x_0 = 0.5a$ )

For every point of nanoplate in  $x$ -direction, porosity distribution 1 yields smallest dynamic deflections compared with uniform and non-uniform porosity 2. Thus, the mode shape of a nanoplate dependent on the type of porosity distribution. Also, increasing uniform porosity coefficient yields larger deflections, because of the reduction in stiffness of nanoplate. Therefore, control of porosities is crucial to obtain the best mechanical performance of nanostructures under dynamic loads.

## 6. Conclusions

In this paper, forced vibration behavior of nonlocal strain gradient porous plates was explored by developing a 4-variable plate model in which shear deformation effect is involved without using shear correction factors. Different porosity distributions in the thickness direction were considered. Two scale coefficients were considered better size-dependent modeling of nanoplate. It was found that increasing the nonlocal parameter results in reduction in the resonance frequencies. However, an inverse trend was observed by considering strain gradient effects. The porosity coefficient and type of porosity distribution has a great influence on resonance frequencies and dynamic deflections of porous nanoplates. The maximum resonance frequency was obtained in the case of symmetric porosity distribution. It was concluded that the resonance frequency is bigger for porous nanoplates with larger magnitudes of the Winkler's and Pasternak's constants. However, resonance frequency is not dependent on the dynamic load location and area.

## References

- Atmane, H.A., Tounsi, A., Bernard, F. and Mahmoud, S.R. (2015), "A computational shear displacement model for vibrational analysis of functionally graded beams with porosities", *Steel Compos. Struct., Int. J.*, **19**(2), 369-384.
- Barati, M.R. (2017), "Investigating dynamic response of porous inhomogeneous nanobeams on hybrid Kerr foundation under hygro-thermal loading", *Appl. Phys. A*, **123**(5), 332.
- Barati, M.R. and Zenkour, A. (2017), "A general bi-Helmholtz nonlocal strain-gradient elasticity for wave propagation in nanoporous graded double-nanobeam systems on elastic substrate", *Compos. Struct.*, **168**, 885-892.
- Barati, M.R., Zenkour, A.M. and Shahverdi, H. (2016), "Thermo-mechanical buckling analysis of embedded nanosize FG plates in thermal environments via an inverse cotangential theory", *Compos. Struct.*, **141**, 203-212.
- Becheri, T., Amara, K., Bouazza, M. and Benseddiq, N. (2016), "Buckling of symmetrically laminated plates using  $n$ th-order shear deformation theory with curvature effects", *Steel Compos. Struct., Int. J.*, **21**(6), 1347-1368.
- Besseglier, A., Heireche, H., Bousahla, A.A., Tounsi, A. and Benzair, A. (2015), "Nonlinear vibration properties of a zigzag single-walled carbon nanotube embedded in a polymer matrix", *Adv. Nano Res., Int. J.*, **3**(1), 29-37.
- Chen, D., Yang, J. and Kitipornchai, S. (2015), "Elastic buckling and static bending of shear deformable functionally graded porous beam", *Compos. Struct.*, **133**, 54-61.
- Chen, D., Kitipornchai, S. and Yang, J. (2016), "Nonlinear free vibration of shear deformable sandwich beam with a functionally graded porous core", *Thin-Wall. Struct.*, **107**, 39-48.
- Ebrahimi, F. and Barati, M.R. (2016), "Analytical solution for nonlocal buckling characteristics of higher-order inhomogeneous nanosize beams embedded in elastic medium", *Adv. Nano Res., Int. J.*, **4**(3), 229-249.
- Ebrahimi, F. and Barati, M.R. (2017a), "Through-the-length temperature distribution effects on thermal

- vibration analysis of nonlocal strain-gradient axially graded nanobeams subjected to nonuniform magnetic field”, *J. Thermal Stress.*, **40**(5), 548-563.
- Ebrahimi, F. and Barati, M.R. (2017b), “Porosity-dependent vibration analysis of piezo-magnetically actuated heterogeneous nanobeams”, *Mech. Syst. Signal Process.*, **93**, 445-459.
- Elmerabet, A.H., Heireche, H., Tounsi, A. and Semmah, A. (2017), “Buckling temperature of a single-walled boron nitride nanotubes using a novel nonlocal beam model”, *Adv. Nano Res., Int. J.*, **5**(1), 1-12.
- Eltaher, M.A., Khater, M.E., Park, S., Abdel-Rahman, E. and Yavuz, M. (2016), “On the static stability of nonlocal nanobeams using higher-order beam theories”, *Adv. Nano Res., Int. J.*, **4**(1), 51-64.
- Eringen, A.C. (1983), “On differential equations of nonlocal elasticity and solutions of screw dislocation and surface waves”, *J. Appl. Phys.*, **54**(9), 4703-4710.
- Jabbari, M., Mojahedin, A., Khorshidvand, A.R. and Eslami, M.R. (2013), “Buckling analysis of a functionally graded thin circular plate made of saturated porous materials”, *J. Eng. Mech.*, **140**(2), 287-295.
- Javed, S., Viswanathan, K.K., Aziz, Z.A., Karthik, K. and Lee, J.H. (2016), “Vibration of antisymmetric angle-ply laminated plates under higher order shear theory”, *Steel Compos. Struct., Int. J.*, **22**(6), 1281-1299.
- Kheroubi, B., Benzair, A., Tounsi, A. and Semmah, A. (2016), “A new refined nonlocal beam theory accounting for effect of thickness stretching in nanoscale beams”, *Adv. Nano Res., Int. J.*, **4**(4), 251-264.
- Li, L. and Hu, Y. (2016), “Wave propagation in fluid-conveying viscoelastic carbon nanotubes based on nonlocal strain gradient theory”, *Computat. Mater. Sci.*, **112**, 282-288.
- Li, L., Li, X. and Hu, Y. (2016a), “Free vibration analysis of nonlocal strain gradient beams made of functionally graded material”, *Int. J. Eng. Sci.*, **102**, 77-92.
- Li, L., Hu, Y. and Ling, L. (2016b), “Wave propagation in viscoelastic single-walled carbon nanotubes with surface effect under magnetic field based on nonlocal strain gradient theory”, *Physica E: Low-dimensional Syst. Nanostruct.*, **75**, 118-124.
- Lim, C.W., Zhang, G. and Reddy, J.N. (2015), “A higher-order nonlocal elasticity and strain gradient theory and its applications in wave propagation”, *J. Mech. Phys. Solids*, **78**, 298-313.
- Mechab, I., Mechab, B., Benaissa, S., Serier, B. and Bouiadjra, B.B. (2016), “Free vibration analysis of FGM nanoplate with porosities resting on Winkler Pasternak elastic foundations based on two-variable refined plate theories”, *J. Brazi. Soc. Mech. Sci. Eng.*, **38**(8), 2193-2211.
- Natarajan, S., Chakraborty, S., Thangavel, M., Bordas, S. and Rabczuk, T. (2012), “Size-dependent free flexural vibration behavior of functionally graded nanoplates”, *Computat. Mater. Sci.*, **65**, 74-80.
- Park, W.T., Han, S.C., Jung, W.Y. and Lee, W.H. (2016), “Dynamic instability analysis for S-FGM plates embedded in Pasternak elastic medium using the modified couple stress theory”, *Steel Compos. Struct., Int. J.*, **22**(6), 1239-1259.
- Reddy, J.N. (1984), “A simple higher-order theory for laminated composite plates”, *J. Appl. Mech.*, **51**(4), 745-752.
- Sobhy, M. and Radwan, A.F. (2017), “A new quasi 3D nonlocal plate theory for vibration and buckling of FGM nanoplates”, *Int. J. Appl. Mech.*, **9**(1), 1750008.
- Tounsi, A., Benguediab, S., Adda, B., Semmah, A. and Zidour, M. (2013), “Nonlocal effects on thermal buckling properties of double-walled carbon nanotubes”, *Adv. Nano Res., Int. J.*, **1**(1), 1-11.
- Wattanasakulpong, N. and Ungbhakorn, V. (2014), “Linear and nonlinear vibration analysis of elastically restrained ends FGM beams with porosities”, *Aerosp. Sci. Technol.*, **32**(1), 111-120.
- Xiao, W., Li, L. and Wang, M. (2017), “Propagation of in-plane wave in viscoelastic monolayer graphene via nonlocal strain gradient theory”, *Appl. Phys. A*, **123**(6), 388.
- Zenkour, A.M. and Abouelregal, A.E. (2015), “Thermoelastic interaction in functionally graded nanobeams subjected to time-dependent heat flux”, *Steel Compos. Struct., Int. J.*, **18**(4), 909-924.
- Zhu, X. and Li, L. (2017), “Closed form solution for a nonlocal strain gradient rod in tension: *International J. Eng. Sci.*”, **119**, 16-28.

**Appendix**

$$\begin{aligned}
 k_{1,1} = & -D \left( \int_0^b \int_0^a \left( \frac{\partial^4 X_m}{\partial x^4} Y_n X_m Y_n \right) dx dy + 2 \int_0^b \int_0^a \left( \frac{\partial^2 X_m}{\partial x^2} \frac{\partial^2 Y_n}{\partial y^2} X_m Y_n \right) dx dy + \int_0^b \int_0^a \left( X_m \frac{\partial^4 Y_n}{\partial y^4} X_m Y_n \right) dx dy \right. \\
 & - \lambda \left( \int_0^b \int_0^a \left( \frac{\partial^6 X_m}{\partial x^6} Y_n X_m Y_n \right) dx dy + 3 \int_0^b \int_0^a \left( \frac{\partial^4 X_m}{\partial x^4} \frac{\partial^2 Y_n}{\partial y^2} X_m Y_n \right) dx dy + 3 \int_0^b \int_0^a \left( \frac{\partial^2 X_m}{\partial x^2} \frac{\partial^4 Y_n}{\partial y^4} X_m Y_n \right) dx dy \right. \\
 & \left. \left. + \int_0^b \int_0^a \left( X_m \frac{\partial^6 Y_n}{\partial y^6} X_m Y_n \right) dx dy \right) - (K_w + K_0) \left( \int_0^b \int_0^a \left( X_m Y_n X_m Y_n \right) dx dy - \mu \left( \int_0^b \int_0^a \left( \frac{\partial^2 X_m}{\partial x^2} Y_n X_m Y_n \right) dx dy \right. \right. \right. \quad (A1) \\
 & \left. \left. + \int_0^b \int_0^a \left( X_m \frac{\partial^2 Y_n}{\partial y^2} X_m Y_n \right) dx dy \right) + K_p \left( \int_0^b \int_0^a \left( \frac{\partial^2 X_m}{\partial x^2} Y_n X_m Y_n \right) dx dy + \int_0^b \int_0^a \left( X_m \frac{\partial^2 Y_n}{\partial y^2} X_m Y_n \right) dx dy \right. \right. \\
 & \left. \left. - \mu \left( \int_0^b \int_0^a \left( \frac{\partial^4 X_m}{\partial x^4} Y_n X_m Y_n \right) dx dy + 2 \int_0^b \int_0^a \left( \frac{\partial^2 X_m}{\partial x^2} \frac{\partial^2 Y_n}{\partial y^2} X_m Y_n \right) dx dy + \int_0^b \int_0^a \left( X_m \frac{\partial^4 Y_n}{\partial y^4} X_m Y_n \right) dx dy \right) \right) \right)
 \end{aligned}$$

$$\begin{aligned}
 k_{2,2} = & -F \left( \int_0^b \int_0^a \left( \frac{\partial^4 X_m}{\partial x^4} Y_n X_m Y_n \right) dx dy + 2 \int_0^b \int_0^a \left( \frac{\partial^2 X_m}{\partial x^2} \frac{\partial^2 Y_n}{\partial y^2} X_m Y_n \right) dx dy + \int_0^b \int_0^a \left( X_m \frac{\partial^4 Y_n}{\partial y^4} X_m Y_n \right) dx dy \right. \\
 & - \lambda \left( \int_0^b \int_0^a \left( \frac{\partial^6 X_m}{\partial x^6} Y_n X_m Y_n \right) dx dy + 3 \int_0^b \int_0^a \left( \frac{\partial^4 X_m}{\partial x^4} \frac{\partial^2 Y_n}{\partial y^2} X_m Y_n \right) dx dy + 3 \int_0^b \int_0^a \left( \frac{\partial^2 X_m}{\partial x^2} \frac{\partial^4 Y_n}{\partial y^4} X_m Y_n \right) dx dy \right. \\
 & \left. \left. + \int_0^b \int_0^a \left( X_m \frac{\partial^6 Y_n}{\partial y^6} X_m Y_n \right) dx dy \right) + A_{44} \left( \int_0^b \int_0^a \left( \frac{\partial^2 X_m}{\partial x^2} Y_n X_m Y_n \right) dx dy + \int_0^b \int_0^a \left( X_m \frac{\partial^2 Y_n}{\partial y^2} X_m Y_n \right) dx dy \right. \right. \\
 & - \lambda \left( \int_0^b \int_0^a \left( \frac{\partial^4 X_m}{\partial x^4} Y_n X_m Y_n \right) dx dy + 2 \int_0^b \int_0^a \left( \frac{\partial^2 X_m}{\partial x^2} \frac{\partial^2 Y_n}{\partial y^2} X_m Y_n \right) dx dy + \int_0^b \int_0^a \left( X_m \frac{\partial^4 Y_n}{\partial y^4} X_m Y_n \right) dx dy \right) \quad (A2) \\
 & - (K_w + K_0) \left( \int_0^b \int_0^a \left( X_m Y_n X_m Y_n \right) dx dy - \mu \left( \int_0^b \int_0^a \left( \frac{\partial^2 X_m}{\partial x^2} Y_n X_m Y_n \right) dx dy + \int_0^b \int_0^a \left( X_m \frac{\partial^2 Y_n}{\partial y^2} X_m Y_n \right) dx dy \right) \right) \\
 & - (N^T + N^H - K_p) \left( \int_0^b \int_0^a \left( \frac{\partial^2 X_m}{\partial x^2} Y_n X_m Y_n \right) dx dy + \int_0^b \int_0^a \left( X_m \frac{\partial^2 Y_n}{\partial y^2} X_m Y_n \right) dx dy - \mu \left( \int_0^b \int_0^a \left( \frac{\partial^4 X_m}{\partial x^4} Y_n X_m Y_n \right) dx dy \right. \right. \\
 & \left. \left. + 2 \int_0^b \int_0^a \left( \frac{\partial^2 X_m}{\partial x^2} \frac{\partial^2 Y_n}{\partial y^2} X_m Y_n \right) dx dy + \int_0^b \int_0^a \left( X_m \frac{\partial^4 Y_n}{\partial y^4} X_m Y_n \right) dx dy \right) \right)
 \end{aligned}$$

$$\begin{aligned}
 m_{1,1} = & +I_0 \left( \int_0^b \int_0^a \left( X_m Y_n X_m Y_n \right) dx dy - \mu \left( \int_0^b \int_0^a \left( \frac{\partial^2 X_m}{\partial x^2} Y_n X_m Y_n \right) dx dy + \int_0^b \int_0^a \left( X_m \frac{\partial^2 Y_n}{\partial y^2} X_m Y_n \right) dx dy \right) \right) \\
 & - I_2 \left( \int_0^b \int_0^a \left( \frac{\partial^2 X_m}{\partial x^2} Y_n X_m Y_n \right) dx dy + \int_0^b \int_0^a \left( X_m \frac{\partial^2 Y_n}{\partial y^2} X_m Y_n \right) dx dy - \mu \left( \int_0^b \int_0^a \left( \frac{\partial^4 X_m}{\partial x^4} Y_n X_m Y_n \right) dx dy \right. \right. \quad (A3) \\
 & \left. \left. + 2 \int_0^b \int_0^a \left( \frac{\partial^2 X_m}{\partial x^2} \frac{\partial^2 Y_n}{\partial y^2} X_m Y_n \right) dx dy + \int_0^b \int_0^a \left( X_m \frac{\partial^4 Y_n}{\partial y^4} X_m Y_n \right) dx dy \right) \right)
 \end{aligned}$$

$$\begin{aligned}
m_{1,2} = m_{2,1} = &+I_0 \left( \int_0^b \int_0^a (X_m Y_n X_m Y_n) dx dy - \mu \left( \int_0^b \int_0^a \left( \frac{\partial^2 X_m}{\partial x^2} Y_n X_m Y_n \right) dx dy + \int_0^b \int_0^a \left( X_m \frac{\partial^2 Y_n}{\partial y^2} X_m Y_n \right) dx dy \right) \right) \\
&-I_4 \left( \int_0^b \int_0^a \left( \frac{\partial^2 X_m}{\partial x^2} Y_n X_m Y_n \right) dx dy + \int_0^b \int_0^a \left( X_m \frac{\partial^2 Y_n}{\partial y^2} X_m Y_n \right) dx dy - \mu \left( \int_0^b \int_0^a \left( \frac{\partial^4 X_m}{\partial x^4} Y_n X_m Y_n \right) dx dy \right. \right. \\
&\left. \left. + 2 \int_0^b \int_0^a \left( \frac{\partial^2 X_m}{\partial x^2} \frac{\partial^2 Y_n}{\partial y^2} X_m Y_n \right) dx dy + \int_0^b \int_0^a \left( X_m \frac{\partial^4 Y_n}{\partial y^4} X_m Y_n \right) dx dy \right) \right) \quad (A4)
\end{aligned}$$

$$\begin{aligned}
m_{2,2} = &+I_0 \left( \int_0^b \int_0^a (X_m Y_n X_m Y_n) dx dy - \mu \left( \int_0^b \int_0^a \left( \frac{\partial^2 X_m}{\partial x^2} Y_n X_m Y_n \right) dx dy + \int_0^b \int_0^a \left( X_m \frac{\partial^2 Y_n}{\partial y^2} X_m Y_n \right) dx dy \right) \right) \\
&-I_5 \left( \int_0^b \int_0^a \left( \frac{\partial^2 X_m}{\partial x^2} Y_n X_m Y_n \right) dx dy + \int_0^b \int_0^a \left( X_m \frac{\partial^2 Y_n}{\partial y^2} X_m Y_n \right) dx dy - \mu \left( \int_0^b \int_0^a \left( \frac{\partial^4 X_m}{\partial x^4} Y_n X_m Y_n \right) dx dy \right. \right. \\
&\left. \left. + 2 \int_0^b \int_0^a \left( \frac{\partial^2 X_m}{\partial x^2} \frac{\partial^2 Y_n}{\partial y^2} X_m Y_n \right) dx dy + \int_0^b \int_0^a \left( X_m \frac{\partial^4 Y_n}{\partial y^4} X_m Y_n \right) dx dy \right) \right) \quad (A5)
\end{aligned}$$

$$Q_{dynamic} = Q_n \left( 1 + \mu \left( \frac{m^2 \pi^2}{a^2} + \frac{n^2 \pi^2}{b^2} \right) \right) \int_0^b \int_0^a (X_m Y_n X_m Y_n) dx dy \quad (A6)$$